Article type: Communication

Visible light actuated efficient exclusion between plasmonic Ag/AgCl micromotors and passive beads

Xu Wang[1], Larysa Baraban[2], Vyacheslav R. Misko[3,4], Franco Nori[4,5], Tao Huang[2], Gianaurelio Cuniberti[2], Jürgen Fassbender[1], and Denys Makarov[1*]*

[1]Helmholtz-Zentrum Dresden-Rossendorf e.V., Institute of Ion Beam Physics and Materials Research, Bautzner Landstrasse 400, 01328 Dresden, Germany

[2]Max Bergmann Center for Biomaterials, Technische Universität Dresden, 01062 Dresden, Germany

[3]TQC, Physics Department, Universiteit Antwerpen, Universiteitsplein 1, B-2610 Antwerpen, Belgium

[4]Theoretical Quantum Physics Laboratory, RIKEN Cluster for Pioneering Research, Wako-shi, Saitama 351-0198, Japan

[5]Physics Department, University of Michigan, Ann Arbor, Michigan 48109-1040, USA

E-mail: d.makarov@hzdr.de, larysa.baraban@nano.tu-dresden.de

Keywords: visible light-driven micromotors, active Janus particles, passive beads, exclusion interaction

We provide insight into the collective behavior of visible-light photochemically driven plasmonic Ag/AgCl Janus particles surrounded by passive Polystyrene (PS) beads. Namely, we analyze, experimentally and in simulations, the active diffusion of single Janus particles and their clusters (small: consisting of two or three Janus particles; and large: consisting of more than ten Janus particles), and their interaction with passive PS beads. The diffusivity of active Janus particles, and thus the exclusive effect to passive PS beads, can be regulated by the number of single Janus particles in the cluster. On the simulation side, we numerically solve the Langevin equations of motion for self-propelled Janus particles and diffusing passive PS beads using Molecular-Dynamics simulations. We consider the complex

interactions of both subsystems, including: elastic core-to-core interactions, short-range attraction, and effective repulsion due to light-induced chemical reactions. This complex mixed system not only provides insight to the interactive effect between active visible light-driven self-propelled micromotors and passive beads, but also offers promise for implications in light-controlled propulsion transport and chemical sensing.

Living systems in nature, like kinesin and myosin, bacteria and fish schools, exhibit dynamic assembling and self-organization when interacting with each other.[1-3] This inspires the design of self-propelled artificial objects that can respond to external stimuli and reveal collective behavior.[4-10] Synthetic nano- and micromotors reveal self-propulsion by converting chemical energy into mechanical motion.[11-16] They interact with their surroundings and realize various scenarios of collective behavior. Being functionalized, artificial machines at various scales have been exposed to interactive environments and used for biomedical applications, like: drug delivery,[17-22] toxin removal,[23, 24] and environmental remediations.[25-29] Recently, light-driven nano/micromotors stimulated research on their fabrication and characterization.[28, 30-40] In photochemically-driven systems, the focus was mainly on various collective behaviors of schooling,[13] oscillation,[12, 41] and assembling.[42] Although fundamentally appealing and relevant for applications to microscale pumping and transport,[43-46] the opposite effect, e.g. exclusion phenomena between active self-propelled micromotors and passive beads are much less explored.

Here, we report on the collective behavior of novel blue-light-actuated plasmonic Ag/AgCl-based Janus micromotors when surrounded by passive PS beads in pure water. The motion of Ag/AgCl-based micromotors is induced by the self-diffusiophoresis mechanism.[13, 40] Thus, when micromotors start moving, a local chemical gradient is generated, changing their

electric potential. These effects contribute to the exclusion behavior of passive beads. The efficiency of exclusion can be improved by increasing the number of single Janus PS/Ag/AgCl particles that compose the cluster. Two reasons contribute to the enhanced effect. On one hand, assemblies with more Janus particles produce stronger chemical gradients and electric potentials. On the other hand, their translational diffusion is drastically depressed due to the passive matrix around, which offers them more interaction time with the surrounding passive beads. This unusual mixture system with exclusion behavior provides insight to design an efficient fuel-free propulsion transfer, from active micromotors to passive beads.

Briefly, the preparation of Janus PS/Ag/AgCl particles is as follows: we assembled a monolayer of 2 μm PS particles and deposited 60 nm Ag layer on top of it. Then a $FeCl_3$/PVP solution (200 mM) was used to oxidize the Ag into Ag/AgCl (details are described in the experimental section). The confirmation of the presence of Ag and AgCl in the cap of a Janus particle is shown in Figure S1 supported by the energy-dispersive X-ray spectroscopy (EDX) analysis. As the hydrophobic metal caps could cause the particles to reorient, interact, and assemble with each other in solution, so that apart from single Janus particles, we could observe the spontaneous formation of various assemblies of single particles (**Figure 1**a-e). The cap of a plasmonic composite Ag/AgCl enables the Janus micromotors to absorb visible light.[4, 47, 48] The motion of Janus PS/Ag/AgCl particles is induced by the self-diffusiophoresis of AgCl in pure H_2O.[13, 40, 41] Single Janus PS/Ag/AgCl micromotors show Brownian motion, and their velocities range from 2 to 7 μm/s under green light illumination (Figure S2a-b). Instead, the velocity is quickly increased (up to 50 to 70 μm/s during its first 2 s) once illuminated with blue light and then gradually decreased down to 10 μm/s in around 7 s (Figure S2c-d).[40] In the following, all time traces for the particles are presented after a

long illumination time, to avoid complications with the transients observed within the first several seconds.

Composites of Ag/AgCl are a well-known plasmonic nanomaterial.[4, 47-50] Here, we rely on this optical property to enable our Janus particles absorbing visible blue light. While pure AgCl-based micromotors move only under UV light illumination[28, 40] as AgCl is a very efficient photocatalyst in the UV[4], the composite Ag/AgCl caps activate the motion of Janus particles under blue light illumination. Upon displacement of a Janus particle, a local chemical gradient is produced, which induces the motion of passive polystyrene beads (Figure 1f).

To study the collective behavior of the blue light-driven Janus particles and their interaction with a passive matrix, we mixed Janus micromotors of different particle assemblies with 1 μm plain PS beads. The experiments are carried out at a sufficiently low concentration of PS beads to avoid any effects of jamming, which could complicate the analysis. Although various assemblies of particles were formed in solution, we further considered three distinct micromotor assemblies composed of one, three, and multiple Janus particles. The trajectories of the Janus particle assemblies as well as of the surrounding PS beads are captured (Figure 2d, 3d, 4d) and analyzed in terms of the mean squared displacement (MSD) (Figure 2e, 3e, 4e) and velocity (Figure 1g). Furthermore, to clearly show the peculiarities of the dynamic properties for each system, we analyze two relevant quantities characterizing the time evolution of the distance between individual PS beads and a Janus micromotor: (i) the distance R between individual PS beads and the moving Janus micromotor (Figure 2f, 3f, 4f) and (ii) the distance R_0 between individual PS beads and the initial position of the Janus micromotor (Figures 2g, 3g, 4g). Those dependences are obtained based on the evaluation of the trajectories data shown in Figures 2d, 3d, 4d.

The most straightforward way is to start the analysis of the behavior of a large cluster consisting of many Janus particles. The particles in the cluster are arranged irregularly leading to a rather isotropic distribution of Ag/AgCl caps (**Figure 1**e). In this respect, the system is somewhat similar to the case of AgCl microparticles[13] and AgCl microstars[28]. We note a clear tendency of PS beads to assemble around the cluster under a reference green-light illumination. This is due to the surface charge attraction: the Zeta potential value of PS/Ag/AgCl micromotors is (-27 ± 2.4) mV, which has a lower level of electronegativity than the value of PS beads (-39 ± 0.5) mV. This difference triggers the particles self-assembly process and is similar to the schooling behavior observed for AgCl microparticles.[13] Reference measurements under green light reveal that the Janus cluster and PS beads exhibit Brownian motion with a typical MSD of 1 μm^2 (Figure S4, for cluster) and 4 μm^2 (Figure S3, for passive beads) in 2 s, respectively.

Once the blue light is on, the PS beads are efficiently repelled from the cluster (**Figure 2**a-c and Videos S1 and S2). Due to its structural isotropy and relatively small diffusivity, the large cluster displays a Brownian motion with a relatively small MSD reaching 5 μm^2 in 2 s (Video S1) even under blue light illumination (blue light intensity of (106 ± 1) $\mu W/mm^2$) (Figure S4), similar to the data shown in Figure 2e. We tracked four PS beads located up-down-left-right with respect to the initial position of the Janus cluster (before the blue light is on) (Video S2). The concentration of the products of the photocatalytic reaction near the large cluster is rather high, which stimulates the efficient directed motion of the surrounding PS beads away from the cluster. Those PS beads, which are closer to the cluster (up and right) acquire an MSD of about 35 μm^2 in 2 s, which is slightly higher compared to the other two beads (about 20 μm^2 in 2 s). The PS beads acquire a noticeable radial velocity component of about 4.4 μm/s (speed after the first second) and are propelled to a distance of about 22 μm

in 7 s, away from the initial (R_0 in Figure 2g) but also the final (R in Figure 2f) position of the cluster.

The cluster of 3 Janus particles is less isotropic and shows much higher diffusivity compared to the large cluster. Therefore, its MSD reaches up to about 28 μm^2 in 2 s (**Figure 3**e). The 3-particle cluster leaves the region with surrounding PS beads relatively quickly, within about 4 s (Figure 3a-c and Video S3). Thus, PS beads interact with the 3-particle cluster for a limited time only, which lead to their rather small directed radial displacement of about 8 μm in 7 s from the initial location of the Janus cluster (R_0 in Figure 4g and Video S4). This is about 2.5 times smaller than in the case of the large cluster (compare Figure 6e and 6f). However, the more efficient motion of a 3-particle cluster increases the value of R up to 16 μm, which is about 1.5x larger than for the case of a Janus cluster (compare Figure 2g and 3g). Furthermore, the MSD of the PS beads is about 10 μm^2 in 2 s (independent of their initial position with respect to the cluster), Figure 3e.

The interaction of a single Janus micromotor with PS beads is very different compared to the case of clusters discussed above. From the experiments, we conclude that the chemical gradient around a single Janus motor is not strong enough to affect the Brownian motion of the PS beads. The only type of interaction is the mechanical impact (i.e., core-to-core interaction) when the Janus motor collides with a PS bead (**Figure 4**a-c and Videos S1). In this case, the bead acquires a directed push from the Janus motor and moves together with the motor as long as they stay in contact. The single Janus micromotor shows a linear trajectory (Figure 4d) with an MSD of about 55 μm^2 in 2 s (Figure 4e and Video S5). This efficient motion allows a single Janus micromotor to leave the interaction region within the first second and minimizes the propulsion effect to the surrounding PS beads. In this case, independent of their initial position with respect to the single Janus particle, the PS beads

almost do not move away from the initial position of the Janus particle (R_0 barely changes in 7 s, Figure 4g). Under blue light illumination, the PS beads perform a Brownian motion with an MSD of about 5 μm^2 in 2 s, which is only slightly higher than the reference MSD value of about 4 μm^2 in 2 s (green light) (Video S6). The increase of the distance R between the Janus micromotor and PS beads is due to the displacement of the Janus particle (Figure 4f). We note that typically only one PS bead acquired a noticeable directed displacement with an MSD of about 12 μm^2 in 2 s (Figure 4e). However, this is a result of a collision of the Janus micromotor into this PS bead (Figure 4e).

Discussion

We model the experiments with single Janus particles and their three- or many-particle assemblies (details can be found below, in the Section "Simulations"). For the case when there is no asymmetric distribution of chemical products around a Janus particle (the reference case of green light illumination in the experiment), Janus particles and their assemblies undergo thermal Brownian diffusion. Turning blue light on initiates the chemical reaction at the Ag/AgCl-covered surface of the Janus particle, which leads to a strong radial flow of the chemical-reaction products from the surface. This flow is responsible for the self-propulsion of the Janus particles and their assemblies, as well as for their long-range interaction with passive beads.

In the experiment, 1 μm PS beads are used, i.e., their translational diffusion coefficient is twice of that for single Janus particles: $D_{T,PS} = 2D_T$, as D_T is inversely proportional to the radius R_P of the particle, $D_T = k_B T/6\pi\eta R_P$.[16] The strength of the flow is an unknown parameter, which we denote by λ. This parameter characterizes the maximum effective force exerted on PS beads at the surface of a Janus particle when illuminated with blue light. This effective force includes contributions from the flow of the fluid and products of the chemical

reaction as well as the electrostatic interactions with (moving) H^+ and Cl^- ions and can hardly be evaluated analytically. Instead, λ is determined via calibration of the simulated MSD on the corresponding experimental data for a single Janus particle (**Figure 4**h, 4i and Figure S5). This behavior is perceived also for the cases when an active Janus particle is fixed at the surface and surrounded by a dense matrix of passive colloidal particles (Figure 5).

A similar situation, for clusters consisting of three single Janus particles, is presented in **Figure 3**h, i. Note that since Janus particles in a three-particle configuration are linked by their hydrophobic Ag/AgCl caps (Figure 1d), their resulting self-propelled velocity is always lower than the self-velocity of a single Janus particle: $v_d < v$. This is explained by the inside orientation of individual Janus particles due to their hydrophobic Ag/AgCl caps, resulting in cancelling out the self-velocities of the constituent individual micromotors. Our estimates show that the self-propelled velocity of a 3-particle Janus assembly, corresponding to the experimentally measured MSD, is typically $v_d \approx 0.4v$ (although v_d can be very small for "antisymmetric" configurations or close to v for rare nearly-symmetric alignment of Janus particles in a two-particle molecule). At the same time, three-particle configurations reveal a much stronger ability to rotate, due to the geometrical arrangement of the caps, which can be seen in their trajectories shown in Figure S6a, 6c, 6e. Similar behavior has been demonstrated earlier for hydrogen peroxide driven two- and three Janus particles assemblies.[62]

Finally, large clusters of Janus particles show even less ability to self-propel, due to the random orientation of individual particles in the clusters. Also, their translational diffusion coefficient scales as $1/R_{cl}$, where R_{cl} is the radius of the cluster. However, thanks to many "engines" that produce a strong flow under blue light, large clusters repel PS beads much stronger than individual (or triple) Janus particles (Video S5, S6). Figure S7 shows the results of simulations of this experimentally observed behavior of large clusters of Janus particles.

Using the flow strength (parameter γ defined above) as a coefficient in the effective repulsion between light-activated clusters and PS beads, calibrated on the experimental values of the MSD for single Janus particles, we evaluated the average distances: (i) between PS beads and Janus particles (also triple, and clusters) and (ii) between PS beads and the initial position of the Janus particle (cluster). The average distances (averaged over several realizations of trajectories of Janus particles and all PS beads in the system) as a function of time are summarized in **Figure 6**. As follows from Figure 6, the distance between a single Janus particle and PS beads is the largest. This is because of the high self-velocity of single Janus particles which escape the collision point (i.e., the initial point where the Janus particle was located when blue light was turned on), thanks to their own engine. While PS beads themselves travel the smallest distance, as the flow produced by a single Janus particle is the smallest. When increasing the number of Janus particles in the assembly (double and triple Janus particles), the distance to moving Janus particles decreases while the distance to the collision point increases. Finally, for large clusters the difference between the two distances becomes very small since large clusters just slightly diffuse away from the collision point. However, this average distance becomes large enough thanks to the strong flow due to the chemical reaction at the surface of many Janus particles in the cluster. Thus, this distance is larger than that for double and triple Janus particles for short times (about 8 s) and is comparable to that for double Janus particles for some longer times. These results agree with our experimental observations.

In summary, we observed new aspects of the collective behavior in a system of visible light-driven active Ag/AgCl Janus micromotors (single, double, triple, and clusters) and passive PS beads, in pure water. When illuminated by visible light, the Janus micromotors perform self-propelled motion and exclude the surrounding PS beads. The exclusion effect to the passive PS beads was found to be much stronger for large assemblies of Janus particles

than for individual Janus micromotors, due to strong flows of the products of the chemical reaction from large clusters. These enhanced flows were detected by tracking the trajectories, average distances, and MSD of the passive beads with respect to the initial position of the Janus particle assemblies (before boosting the chemical reaction at the surface of Ag/AgCl-based micromotors by blue light) and to the position of the moving Janus particle or cluster. The observed collective behavior was also analyzed in simulations, by numerically solving the Langevin equations of motion for active Janus motors (and their clusters) in the presence of diffusing passive beads. While basic parameters of the model, such as the diffusion constants, were evaluated theoretically, the unknown interaction parameters between active motors and passive beads were determined via calibration with the available experimental data. The results of the simulations are in agreement with the observations and shed light on the complex dynamics of the interacting active-passive system. The observed efficient visible light-driven exclusion in the mixed system of active micromotors and passive beads could be further applied for biological studies, such as the investigation of the interaction between motile micromotors and bio objects.

Experimental Section

Fabrication of Janus Polystyrene/Ag/AgCl micromotors: Self-assembled monolayers of 2 μm polystyrene (PS) particles were prepared by drop casting the PS suspension (25 mg/mL in Ethanol solution) onto O_2 plasma pre-processed glass slides. After the process of electron beam deposition (base pressure: 7×10^{-7} mbar; deposition rate of 1 nm/s), a 60 nm thick Ag layer was on the upper surface of the PS monolayer. Then the Janus Ag coated polystyrene particles (PS/Ag) were resuspended in DI (deionized) water and were dispersed in a polyvinylpyrrolidone (PVP) solution (50 mM) by a sonication process. Afterwards, an excess

$FeCl_3$ solution (0.02 M) was added to it and stirred for 20 min. The final solution was washed with DI water for five times and suspended in DI water for future use. The whole synthesis process must be done in a dark environment. The propulsion of micromotors in deionized (DI) water is due to the photocatalytic reduction of AgCl[51] at the location of the cap: $4AgCl + 2H_2O \rightarrow 4Ag + 4H^+ + 4Cl^- + O_2\bullet^-$.

Materials and Instruments: The PVP (Mw = 55000), Iron(III) chloride hexahydrate ($FeCl_3\bullet 6H_2O$) and the Polystyrene microparticles (diameters: 1 μm and 2 μm) are from Sigma-Aldrich. The 4-wavelength LED lamp and its driver (DC4104) are from THORLABS and the fluorescence lamp (HBO 103) is from Carl Zeiss Microscope. The light power detector (XLP 12) and its monitor are from Gentec-eo. The specimens for SEM were prepared by drop casting a 0.002 ml microparticle solution on a 5 mm x 5 mm Si wafer and coating it with a 20 nm thick carbon layer (SCD500 coater, Leica Microsystems GmbH, Germany) to reduce charging of the specimen in the electron beam. The SEM images were acquired in Ultra Plus (Carl Zeiss Microscopy GmbH, Germany) SEM operated at 3 kV.

Optical video recording: The motion of Janus PS/Ag/AgCl particles and 1 μm PS beads were recorded with a Carl Zeiss inverted microscope (Axiovert 200 M) integrated with a Cascade video camera (5120). The suspension with Janus micromotors was diluted and mixed on a clean glass slide with a droplet of DI water. To study the collective behavior, a suspension with PS beads was dispersed in a DI water droplet and then it was further diluted in the suspension with Janus PS/Ag/AgCl particles. 400 frames video files were recorded with a Cascade camera (28 frames/s). Two kinds of light illuminations were used for video recordings.

Green light illumination: For reference measurements, we used the bright light from the microscope lamp (12 V and 100 W Halogen lamp), which was processed by the filter sets in

green and yellow colors. Thus, we obtain a green-colored light, which is used here as a reference. The intensity of the reference green light is (8 ± 1) μW /mm^2.

Blue light illumination: The source of blue light was provided by the external fluorescence lamp with Zeiss filter sets, which is typically used for high quality fluorescence experiments. It has an excitation wavelength of 450-490 nm and an emission wavelength of 515 nm. The blue light intensity is (106 ± 1) μW/mm^2. All the light intensities were measured with a light power detector (gentec-eo XLP 12).

Video analysis: Custom scripts in Python using the OpenCV library and TrackMate from the image processing software Fiji (http://fiji.sc/) were used for particle tracking to obtain the trajectory data (x,y) coordinates of Janus PS/Ag/AgCl particles and their assemblies. The MSD was calculated as follows: MSD = $[r(t + \Delta t) - r(t)]^2_t$ with Δt the time step between video frames and r the (x,y) coordinate values from individual video tracking.[52, 53] Following the classical works on the evaluation of the MSD,[54] we present MSD data up to 2 s only based on the information obtained from a 7 s long tracking movie (about 1/4 of the total duration of the tracking movie). In addition, in Figure S8, we show the experimental and simulated 7-s-long MSD curves of the micromotors (cluster, 3-particles assembly, and single Janus particle) and their surrounding PS beads.

Simulations: The motion of active micromotors characterized by the self-propelled velocity v as well as passive beads with $v = 0$ was simulated by numerically integrating the following overdamped Langevin equations: [55-59]

$$\begin{aligned} \dot{x}_i &= v_0 \cos\theta_i + \xi_{i0,x}(t) + \sum_{ij}^{N} f_{ij,x}, \\ \dot{y}_i &= v_0 \sin\theta_i + \xi_{i0,y}(t) + \sum_{ij}^{N} f_{ij,y}, \\ \dot{\theta}_i &= \xi_{i\theta}(t), \end{aligned} \qquad (1)$$

for i,j running from 1 to the total number N of particles, active and passive, in the system. Here, μ is the mobility of Janus particles, $\xi_{i0}(t) = (\xi_{i0,x}(t), \xi_{i0,y}(t))$ is a two-dimensional (2D) thermal Gaussian noise with correlation functions $\langle \xi_{0,\alpha}(t) \rangle = 0$, $\langle \xi_{0,\alpha}(t)\xi_{0,\beta}(t) \rangle = 2D_T\delta_{\alpha\beta}\delta(t)$, where $\alpha,\beta = x,y$, and D_T is the translational diffusion constant of a passive particle of the same geometry as an active micromotor, at a fixed temperature; $\xi_\theta(t)$ is an independent 1D Gaussian noise with correlation functions $\langle \xi_\theta(t) \rangle = 0$ and $\langle \xi_\theta(t)\xi_\theta(0) \rangle = 2D_R\delta(t)$ that models the fluctuations of the propulsion angle θ. The diffusion coefficients D_T and D_R can be directly calculated[60] or extracted from experimentally measured trajectories and MSD, by fitting to theoretical MSD.[16] Thus, for a particle with radius $R_P = 1$ μm diffusing in water at room temperature, the corresponding translational diffusion coefficient is $D_T \approx 0.22$ μm^2/s, and the rotational diffusion coefficient is $D_R \approx 0.16$ rad^2/s.[61] We adopt these values in our model.

The last term in the first two equations, $\sum_{ij}^{N} f_{ij}$, represents, in a compact form, the sum of all inter-particle interaction forces in the system. These interactions, in particular, include: (i) elastic soft-core repulsive interactions between active particles, between passive beads, as well as between active and passive particles;[55-59] (ii) the experimentally observed short-range attraction among particles leading to their aggregation in "molecules" and clusters;[57, 62, 63] and (iii) effective repulsive interaction between Janus particles and passive beads, due to the radial flow of products of chemical reaction from the surface of Ag/AgCl Janus particles when being illuminated by blue light.

The interaction between particles of any sort, active or passive, during the collisions, i.e., the core-to-core interaction, is modeled by an elastic repulsive force:[55-59]

$$f_{ij}^{rep} = \begin{cases} k(R_i + R_j - |\vec{r}_i - \vec{r}_j|), & if\ |\vec{r}_i - \vec{r}_j| < R_i + R_j, \\ 0, & if\ |\vec{r}_i - \vec{r}_j| \geq R_i + R_j, \end{cases} \quad (2)$$

where $R_{i,j}$ and $\vec{r}_{i,j}$ are, correspondingly, the radius and the position of the $i(j)$th particle, and k is the spring constant of the elastic repulsive interaction. The experimentally observed adhesion among Janus particles and silica beads[57, 62, 63] (due to the electrostatic attraction and possibly other mechanisms) is modeled by an additional effective short-range attractive force term:

$$f_{ij}^{att} = \begin{cases} \dfrac{\kappa(R_i R_j)}{|\vec{r}_i - \vec{r}_j|^2}, & if\ |\vec{r}_i - \vec{r}_j| > R_i + R_j, \\ 0, & if\ |\vec{r}_i - \vec{r}_j| >> R_i + R_j, \end{cases} \quad (3)$$

where κ is a tunable coefficient for the attractive interaction. This attractive interaction results, in particular, in the aggregation of Janus particles in two- and three- particle "molecules" and in large clusters, as well as in the adhesion of PS beads to Ag/AgCl particles and the formation of irregular "shells" of PS beads around Ag/AgCl particles and their aggregates. Note that the chemical reaction at the surface of Ag/AgCl particles induced by blue light creates a strong radial flow of the ions and other particles from the surface of the particles. This flow easily overcomes the attraction between the Ag/AgCl particles (or their aggregates) and PS beads and strongly repels the PS beads away from the Ag/AgCl particles, as observed in experiments. This repulsion depends on the number of Ag/AgCl particles in the aggregates. Thus, large clusters of Ag/AgCl Janus particles repel PS beads much stronger than single Janus particles when illuminated by blue light. We model this radial flow by a finite-range field of radial forces, decreasing in amplitude as $1/r$ from the center of a cluster of Janus particles (or a single particle):

$$f_{ij}^{flow} = \begin{cases} \dfrac{\gamma}{\left|\vec{r}_i - \vec{r}_j\right|}, & if\ \left|\vec{r}_i - \vec{r}_j\right| > R_i + R_j, \\ 0, & if\ \left|\vec{r}_i - \vec{r}_j\right| >> R_i + R_j, \end{cases} \quad (4)$$

where γ is the cumulative "strength of the flow" parameter, which includes the flow of the fluid, the gradient of the concentration profile of ions (note that negative ions repel negatively charged PS beads) and other products of the chemical reaction from the surface of the AgCl particles[64] illuminated by blue light. The parameter γ is determined from the calibration of the simulated trajectories and the MSD of the PS beads to the experimentally measured MSD, for the case of a single Ag/AgCl Janus particle, and, respectively, varied for double, triple Janus particles and their large clusters. Thus, we found that for single Janus particles $\mu\gamma \approx$ (3.2 - 3.9) $\mu m^2/s$, and for clusters $\mu\gamma \approx$ (19.4 - 27.2) $\mu m^2/s$.

The simulation procedure includes two main steps. On the first step, the initial state of the system is prepared so that it corresponds to the moment of time right before the blue light is turned on. A single Ag/AgCl Janus particle or cluster of Janus particles was placed at the position (0,0), and other particles, i.e., PS beads, were distributed randomly. During the first 400 s of the simulation, the particles executed Brownian motion. As a result, some PS beads aggregated near the Janus particle (or the cluster of Janus particles) and some PS beads were located away from the Janus particle. Then the repulsive interaction (4) was turned on, so that models turning on the blue light in the experiment, the self-propelled particles acquired a self-velocity $v > 0$, and the trajectories of all the particles including the Janus particle (or cluster) and PS beads were recorded; typically, during the first 10 s (corresponding to typical experimental observation times).

Supporting Information:

Supporting Information is available from the Wiley Online Library or from the author. The file includes further details on measured and simulated trajectories of Janus particles. The corresponding velocities of the particles as well as the MSD data are presented as well.

Video S1. (for Figure 4a-c) Trajectory recordings of a single Janus PS/Ag/AgCl particle surrounded by 1 μm PS beads under green and blue light illumination.

Video S2. (for Figure 4d-g) Trajectory recordings of four PS beads around a single Janus PS/Ag/AgCl micromotor under blue light illumination.

Video S3. (for Figure 3a-c) Trajectory recordings of 3-particles Janus surrounded by 1 μm PS beads under green and blue light illumination.

Video S4. (for Figure 3d-g) Trajectory recordings of four PS beads around a 3-particles Janus under blue light illumination.

Video S5. (for Figure 2a-c) Trajectory recordings of a Janus cluster surrounded by 1 μm PS beads under green and blue light illumination.

Video S6. (for Figure 2d-g) Trajectory recordings of PS beads around a Janus cluster under blue light illumination.

Author Contributions

DM, XW, and LB formulated the task. XW carried out experimental work with the contribution from TH, and LB. VRM performed simulations and analyzed the data with contributions from FN. The manuscript was written by XW, DM, LB, and VRM with contributions from GC, JF, and FN. All authors have given approval to the final version of the manuscript.

Acknowledgements

We thank P. Formanek (Leibniz-Institut für Polymerforschung Dresden) for support with the SEM measurements, B. Ibarlucea (TU Dresden) for Zeta potential measurements, J. Grenzer and A. Scholz (HZDR) for x-ray diffraction characterization. The participation of J. Tempere (Universiteit Antwerpen), A. Nguyen (TU Dresden), J. Ge (HZDR) at the initial stage of the project is greatly acknowledged. Support by the Nanofabrication Facilities Rossendorf and Structural Characterization Facilities Rossendorf at the Ion Beam Center (IBC) at the HZDR is greatly appreciated. The work was financially supported in part *via* the German Research Foundation (DFG) Grant MA 5144/9-1. V.R.M. acknowledges support from the Research Foundation - Flanders (FWO-Vl), and F.N. acknowledges support from the Japan Society for the Promotion of Science (JSPS), *via* the FWO-JSPS bilateral grant No. VS.059.18N. F.N. is supported in part by the MURI Center for Dynamic Magneto-Optics via the Air Force Office of Scientific Research (AFOSR) (FA9550-14-1-0040), Army Research Office (ARO) (Grant No. 73315PH), Asian Office of Aerospace Research and Development (AOARD) (Grant No. FA2386-18-1-4045), Japan Science and Technology Agency (JST) (the ImPACT program and CREST Grant No. JPMJCR1676), JSPS (JSPS-RFBR Grant No. 17-52-50023), RIKEN-AIST Challenge Research Fund, and the John Templeton Foundation.

Abbreviations

MSD mean squared displacements; UV ultraviolet; PS polystyrene; DI deionized; PVP polyvinylpyrrolidone; SEM scanning electron microscopy.

REFERENCES

[1] H. P. Zhang, A. Be'er, E. L. Florin, H. L. Swinney, *Proc. Natl. Acad. Sci. U. S. A.* **2010**, 107, 13626.

[2] M. C. Marchetti, J. F. Joanny, S. Ramaswamy, T. B. Liverpool, J. Prost, M. Rao, R. A. Simha, *Rev. Mod. Phys.* **2013**, 85, 1143.

[3] A. P. Petroff, X. L. Wu, A. Libchaber, *Phys. Rev. Lett.* **2015**, 114, 158102.

[4] P. Wang, B. B. Huang, X. Y. Qin, X. Y. Zhang, Y. Dai, J. Y. Wei, M. H. Whangbo, *Angew. Chem., Int. Ed.* **2008**, 47, 7931.

[5] A. Bricard, J. B. Caussin, N. Desreumaux, O. Dauchot, D. Bartolo, *Nature* **2013**, 503, 95.

[6] J. Palacci, S. Sacanna, A. P. Steinberg, D. J. Pine, P. M. Chaikin, *Science* **2013**, 339, 936.

[7] W. Wang, W. Duan, S. Ahmed, A. Sen, T. E. Mallouk, *Acc. Chem. Res* **2015**, 48, 1938.

[8] J. Stenhammar, R. Wittkowski, D. Marenduzzo, M. E. Cates, *Sci. Adv* **2016**, 2, e1501850.

[9] J. Yan, M. Han, J. Zhang, C. Xu, E. Luijten, S. Granick, *Nat. Mater* **2016**, 15, 1095.

[10] C. Chen, X. Chang, H. Teymourian, D. E. R. Herrera, B. E. Fernández de Ávila, X. Lu, J. Li, S. He, C. Fang, Y. Liang, *Angew. Chem., Int. Ed.* **2018**, 57, 241.

[11] L. Baraban, D. Makarov, R. Streubel, I. Mönch, D. Grimm, S. Sanchez, O. G. Schmidt, *ACS nano* **2012**, 6, 3383.

[12] A. Altemose, M. A. Sanchez-Farran, W. Duan, S. Schulz, A. Borhan, V. H. Crespi, A. Sen, *Angew. Chem., Int. Ed.* **2017**, 56, 7817.

[13] M. Ibele, T. E. Mallouk, A. Sen, *Angew. Chem., Int. Ed*. **2009**, 48, 3308.

[14] Y. Mei, A. A. Solovev, S. Sanchez, O. G. Schmidt, *Chem. Soc. Rev.* **2011**, 40, 2109.

[15] L. Baraban, D. Makarov, O. G. Schmidt, G. Cuniberti, P. Leiderer, A. Erbe, *Nanoscale* **2013**, 5, 1332.

[16] J. R. Howse, R. A. L. Jones, A. J. Ryan, T. Gough, R. Vafabakhsh, R. Golestanian, *Phys. Rev. Lett.* **2007**, 99, 048102.

[17] V. Garcia Gradilla, S. Sattayasamitsathit, F. Soto, F. Kuralay, C. Yardimci, D. Wiitala, M. Galarnyk, J. Wang, *Small* **2014**, 10, 4154.

[18] Z. Wu, X. Lin, X. Zou, J. Sun, Q. He, *ACS Appl. Mater. Interfaces* **2015**, 7, 250.

[19] X. Ma, K. Hahn, S. Sanchez, *J. Am. Chem. Soc.* **2015**, 137, 4976.

[20] F. Peng, Y. Tu, J. van Hest, D. A. Wilson, *Angew. Chem., Int. Ed.* **2015**, 127, 11828.

[21] C. Peters, M. Hoop, S. Pane, B. J. Nelson, C. Hierold, *Adv. Mater* **2016**, 28, 533.

[22] B. E.-F. de Ávila, P. Angsantikul, J. Li, M. A. Lopez-Ramirez, D. E. Ramírez-Herrera, S. Thamphiwatana, C. Chen, J. Delezuk, R. Samakapiruk, V. Ramez, *Nat. Commun.* **2017**, 8, 272.

[23] Z. Wu, T. Li, W. Gao, T. Xu, B. Jurado-Sánchez, J. Li, W. Gao, Q. He, L. Zhang, J. Wang, *Adv. Funct. Mater* **2015**, 25, 3881.

[24] B. E.-F. de Ávila, P. Angsantikul, D. E. Ramírez-Herrera, F. Soto, H. Teymourian, D. Dehaini, Y. Chen, L. Zhang, J. Wang, *Sci. Robot.* **2018**, 3, eaat0485.

[25] L. Soler, V. Magdanz, V. M. Fomin, S. Sanchez, O. G. Schmidt, *ACS Nano* **2013**, 7, 9611.

[26] D. A. Uygun, B. Jurado-Sanchez, M. Uygun, J. Wang, *Environ. Sci.: Nano* **2016**, 3, 559.

[27] D. Vilela, J. Parmar, Y. Zeng, Y. Zhao, S. Sanchez, *Nano Lett.* **2016**, 16, 2860.

[28] J. Simmchen, A. Baeza, A. Miguel-Lopez, M. M. Stanton, M. Vallet-Regi, D. Ruiz-Molina, S. Sanchez, *Chemnanomat* **2017**, 3, 65.

[29] K. Villa, J. Parmar, D. Vilela, S. Sanchez, *ACS Appl. Mater. Interfaces* **2018**, 8b04353

[30] B. Dai, J. Wang, Z. Xiong, X. Zhan, W. Dai, C. C. Li, S. P. Feng, J. Tang, *Nat. Nanotechnol.* **2016**, 11, 1087.

[31] R. Dong, Q. Zhang, W. Gao, A. Pei, B. Ren, *ACS Nano* **2016**, 10, 839.

[32] W. Li, X. R. Wu, H. Qin, Z. Q. Zhao, H. W. Liu, *Adv. Funct. Mater* **2016**, 26, 3164.

[33] S. Palagi, A. G. Mark, S. Y. Reigh, K. Melde, T. Qiu, H. Zeng, C. Parmeggiani, D. Martella, A. Sanchez-Castillo, N. Kapernaum, F. Giesselmann, D. S. Wiersma, E. Lauga, P. Fischer, *Nat. Mater* **2016**, 15, 647.

[34] C. Chen, F. Mou, L. Xu, S. Wang, J. Guan, Z. Feng, Q. Wang, L. Kong, W. Li, J. Wang, Q. Zhang, *Adv. Mater.* **2017**, 29, 1603374

[35] R. Dong, Y. Hu, Y. Wu, W. Gao, B. Ren, Q. Wang, Y. Cai, *J. Am. Chem. Soc.* **2017**, 139, 1722.

[36] B. Jang, A. Hong, H. E. Kang, C. Alcantara, S. Charreyron, F. Mushtaq, E. Pellicer, R. Buchel, J. Sort, S. S. Lee, B. J. Nelson, S. Pane, *ACS Nano* **2017**, 11, 6146.

[37] J. Zheng, B. Dai, J. Wang, Z. Xiong, Y. Yang, J. Liu, X. Zhan, Z. Wan, J. Tang, *Nat. Commun.* **2017**, 8, 1438.

[38] D. P. Singh, W. E. Uspal, M. N. Popescu, L. G. Wilson, P. Fischer, *Adv. Funct. Mater* **2018**, 1706660.

[39] X. Wang, V. Sridhar, S. Guo, N. Talebi, A. Miguel-López, K. Hahn, P. A. van Aken, S. Sánchez, *Adv. Funct. Mater* **2018**, 1705862.

[40] C. Zhou, H. P. Zhang, J. Y. Tang, W. Wang, *Langmuir* **2018**, 34, 3289.

[41] M. E. Ibele, P. E. Lammert, V. H. Crespi, A. Sen, *ACS Nano* **2010**, 4, 4845.

[42] D. P. Singh, U. Choudhury, P. Fischer, A. G. Mark, *Adv. Mater* **2017**, 29, 1701328.

[43] J. J. McDermott, A. Kar, M. Daher, S. Klara, G. Wang, A. Sen, D. Velegol, *Langmuir* **2012**, 28, 15491.

[44] A. Afshar Farniya, M. J. Esplandiu, A. Bachtold, *Langmuir* **2014**, 30, 11841.

[45] E. L. Jewell, W. Wang, T. E. Mallouk, *Soft Matter* **2016**, 12, 2501.

[46] M. Li, Y. Su, H. Zhang, B. Dong, *Nano Research* **2018**, 11, 1810.

[47] Y. Bi, J. Ye, *Chem. Commun* **2009**, 6551.

[48] Y. X. Tang, Z. L. Jiang, G. C. Xing, A. R. Li, P. D. Kanhere, Y. Y. Zhang, T. C. Sum, S. Z. Li, X. D. Chen, Z. L. Dong, Z. Chen, *Adv. Funct. Mater* **2013**, 23, 2932.

[49] C. An, S. Peng, Y. Sun, *Adv. Mater* **2010**, 22, 2570.

[50] P. Wang, B. Huang, Z. Lou, X. Zhang, X. Qin, Y. Dai, Z. Zheng, X. Wang, *Chem. - Eur. J.* **2010**, 16, 538.

[51] G. Calzaferri, *Catalysis today* **1997**, 39, 145.

[52] G. Dunderdale, S. Ebbens, P. Fairclough, J. Howse, *Langmuir* **2012**, 28, 10997.

[53] L. Weimann, K. A. Ganzinger, J. McColl, K. L. Irvine, S. J. Davis, N. J. Gay, C. E. Bryant, D. Klenerman, *PLoS One* **2013**, 8, e64287.

[54] M. J. Saxton, *Biophys J* **1997**, 72, 1744.

[55] P. K. Ghosh, V. R. Misko, F. Marchesoni, F. Nori, *Phys. Rev. Lett.* **2013**, 110, 268301.

[56] D. Takagi, A. B. Braunschweig, J. Zhang, M. J. Shelley, *Phys. Rev. Lett.* **2013**, 110, 038301.

[57] H. Yu, A. Kopach, V. R. Misko, A. A. Vasylenko, D. Makarov, F. Marchesoni, F. Nori, L. Baraban, G. Cuniberti, *Small* **2016**, 12, 5882.

[58] P. K. Ghosh, P. Hänggi, F. Marchesoni, F. Nori, *Phys. Rev. E* **2014**, 89, 062115.

[59] W. Yang, V. R. Misko, F. Marchesoni, and F. Nori, J. Phys.: Condens. Matter **2018**, 30, 264004.

[60] E. Purcell, *Am. J. Phys.* **1977**, 45, 3.

[61] G. Volpe, S. Gigan, G. Volpe, *Am. J. Phys.* **2014**, 82, 659.

[62] S. Ebbens, R. A. Jones, A. J. Ryan, R. Golestanian, J. R. Howse, *Phys. Rev. E* **2010**, 82, 015304.

[63] L. Baraban, M. Tasinkevych, M. N. Popescu, S. Sanchez, S. Dietrich, O. G. Schmidt, *Soft Matter* **2012**, 8, 48.

[64] R. Golestanian, *Phys. Rev. Lett.* **2009**, 102, 188305.

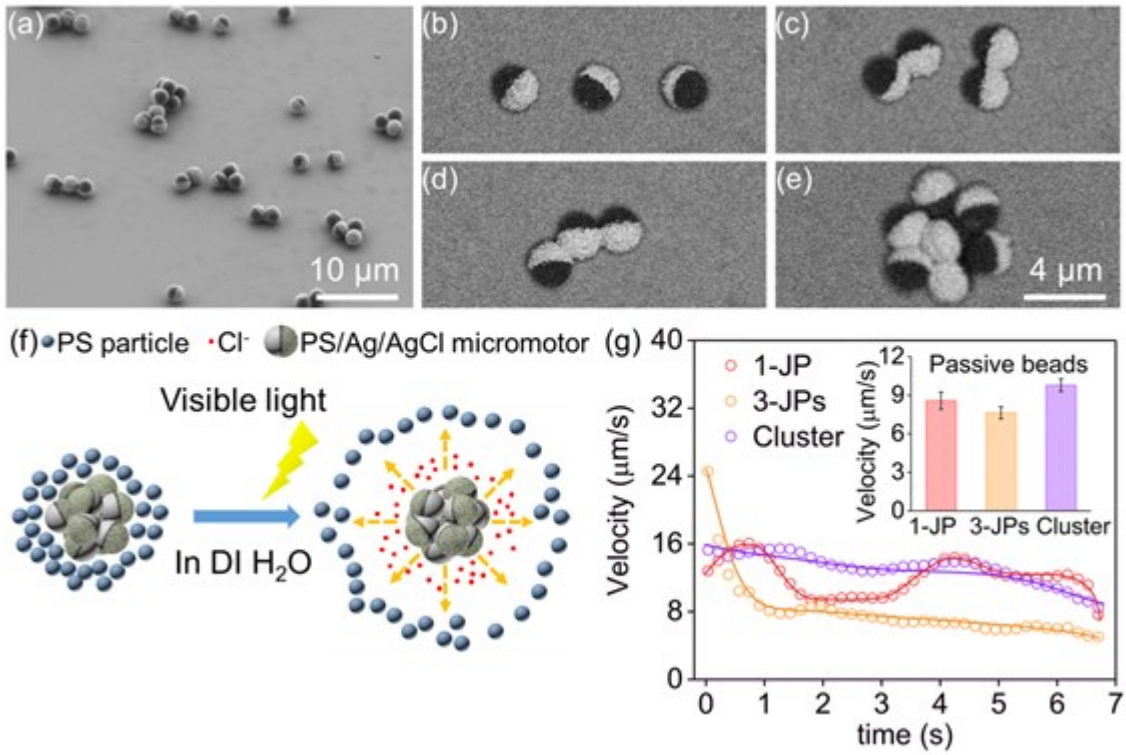

Figure 1. (a-e) SEM image of 1- , 2-, 3-particles assemblies and a cluster. (f) Schematic figure of blue light actuated exclusion process between a PS/Ag/AgCl cluster and surrounding passive PS particles in pure H_2O. (g) Velocity of 1-, 3-particles assemblies and a cluster, together with the fitted guiding lines for each colored symbol. The corresponding velocities of the surrounding passive PS beads, averaged over four of them for each of the assemblies, are shown with colored columns in the inset.

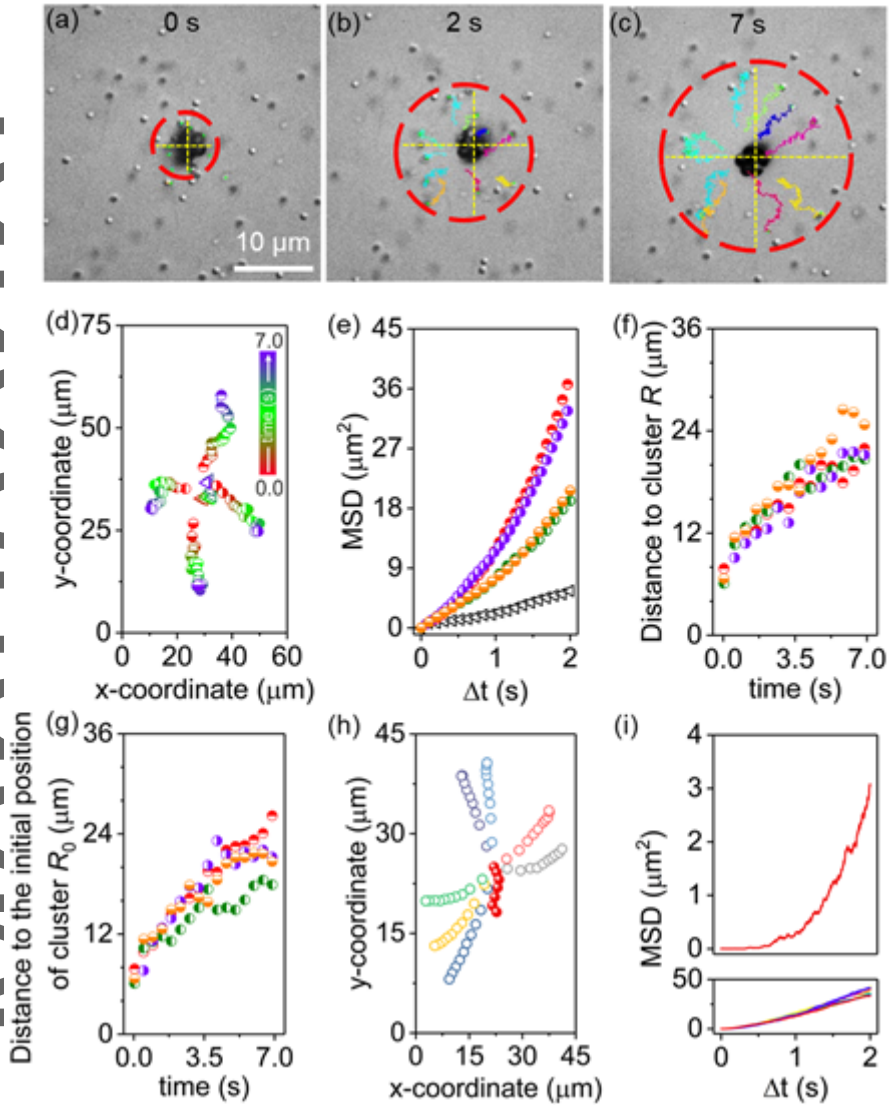

Figure 2. (a-c) A sequence of video snapshots showing the motion of a self-propelled cluster consisting of around 30 Janus PS/Ag/AgCl particles and the exclusive effect to nearby passive PS beads under blue light illumination [(106 ± 1) μW/mm^2]. (d) Trajectories of the cluster (open triangles) and surrounding passive PS beads (half-open circles). The measurement is taken over 7 s under blue light illumination [(106 ± 1) μW/mm^2]. (e) The corresponding experimental MSD curves of the cluster (black triangles) and surrounding PS beads (color symbols). The orientation of the filled part of the symbols correlates with the data shown in panel (d). (f) Distance R between a PS bead and the Janus cluster. (g) Distance R_0 between a PS bead and the initial position of the cluster. (h) Simulated trajectories over 7 s of a Janus cluster (v = 0.9 μm/s; closed symbols) surrounded with PS beads (open symbols). (i) The corresponding simulated MSD curves of the cluster (top panel) and surrounding passive PS beads (bottom panel) in 2 s.

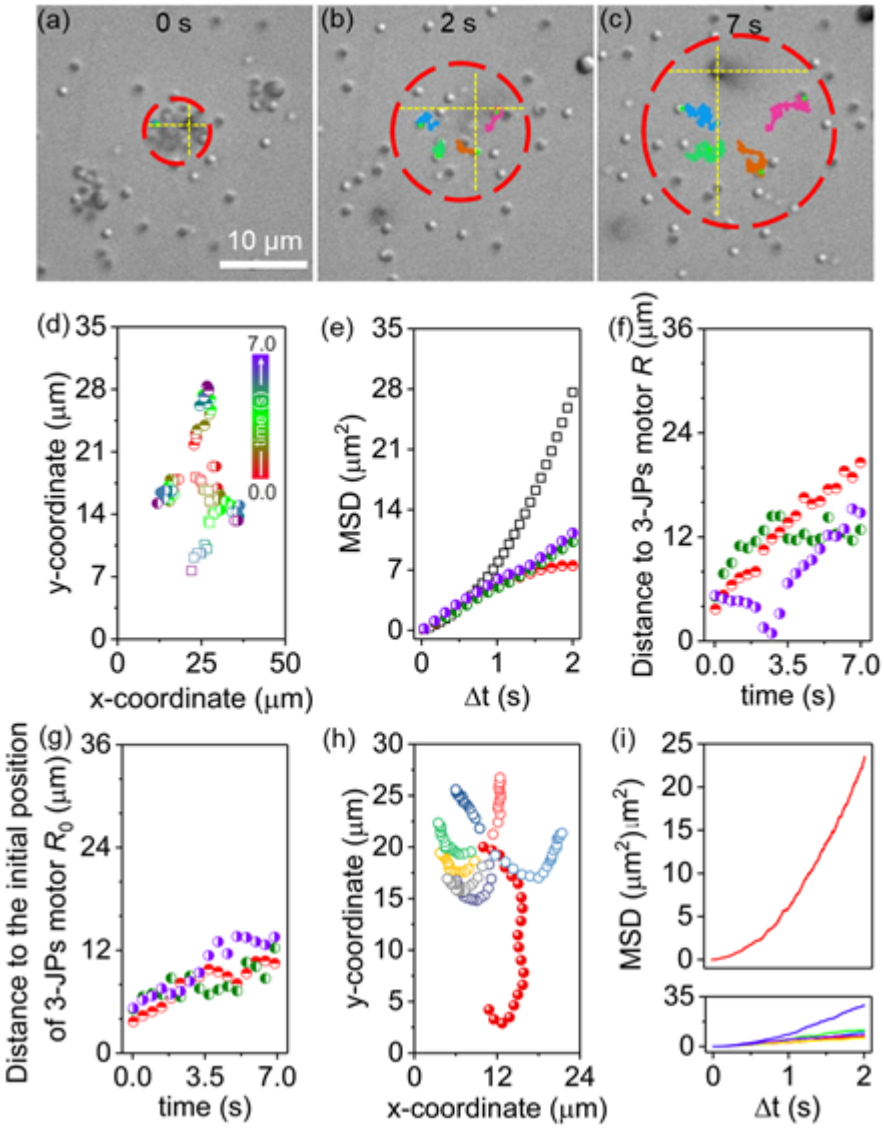

Figure 3. (a-c) A sequence of video snapshots showing the motion of a self-propelled 3-particles assembly and the exclusive effect to nearby passive PS beads under blue light illumination [(106 ± 1) μW/mm^2]. (d) Trajectories of the 3-particles assembly (open squares) and surrounding passive PS beads (half-open circles) under blue light illumination [(106 ± 1) μW/mm^2]. (e) The corresponding experimental MSD curves of the 3-particles assembly (black squares) and surrounding PS beads (color symbols). The orientation of the filled part of the symbols correlates with the data shown in panel (d). (f) Distance R between a PS bead and the 3-particles assembly. (g) Distance R_0 between a PS bead and the initial position of the 3-particles assembly. (h) Simulated trajectories over 7 s of a 3-particles assembly (v = 2.5 μm/s; closed symbols) surrounded by PS beads (open symbols). (i) The corresponding simulated MSD curves of the 3-particles assembly (top panel) and surrounding passive PS beads (bottom panel) in 2 s.

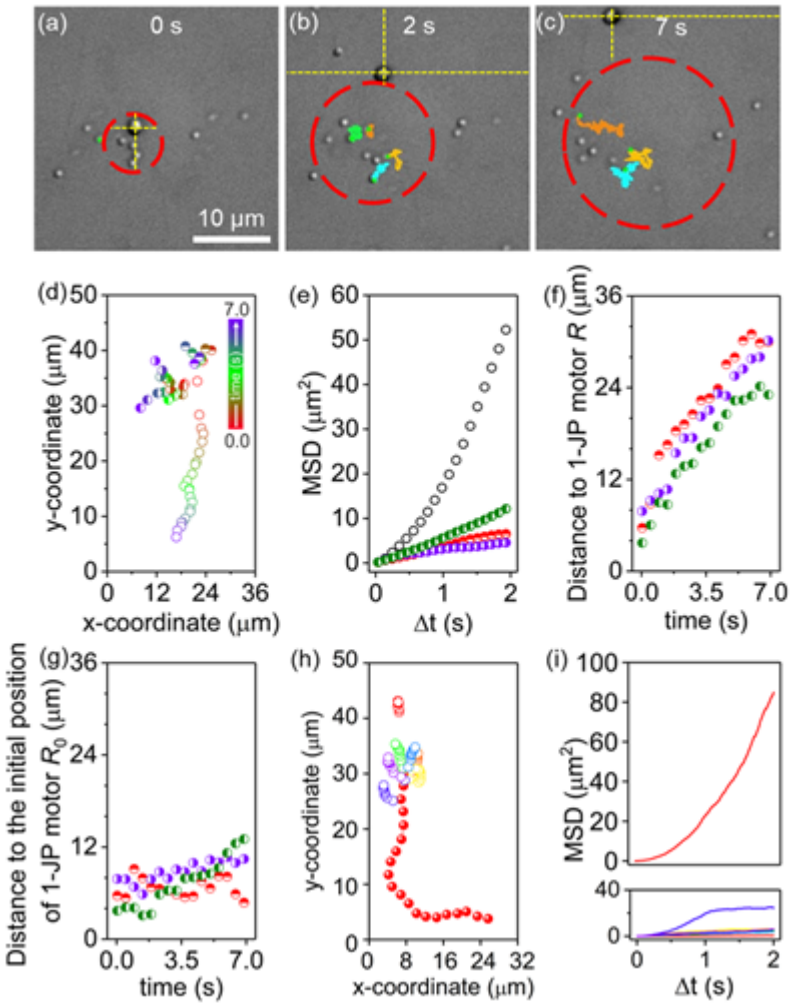

Figure 4. (a-c) A sequence of video snapshots showing the motion of a self-propelled single Janus particle (open circles in panels (d,e)) and the exclusion effect to nearby passive PS beads under blue light illumination [(106 ± 1) μW/mm^2]. (d) Trajectories of the single Janus particle (open circles) and surrounding passive PS beads (half-open circles) under blue light illumination [(106 ± 1) μW/mm^2]. (e) The corresponding experimental MSD curves of a single Janus particle (black circles) and surrounding PS beads (color symbols). The orientation of the filled part of the symbols correlates with the data shown in panel (d). (f) Distance R between PS beads and the single Janus particle. (g) Distance R_0 between PS beads and the initial position of the single Janus particle. (h) Simulated trajectories over 7 s of a single Janus particle (v = 5 μm/s; closed symbols) surrounded by PS beads (open symbols). (i) The corresponding simulated MSD curves of the single Janus particle (top panel) and surrounding passive PS beads (bottom panel) in 2 s.

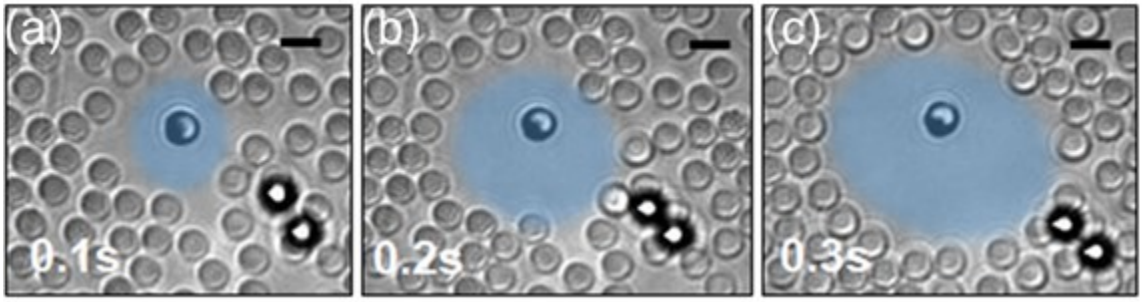

Figure 5. The interaction of a single Janus micromotor, fixed to the surface with the passive matrix for the case of high concentrated passive SiO_2 beads (diameter of 2 μm). Panels from left to right show the time evolution (a) 0.1 s, (b) 0.2 s, and (c) 0.3 s of the radius *R* between the centre of the active Janus micromotor and the surrounding passive beads.

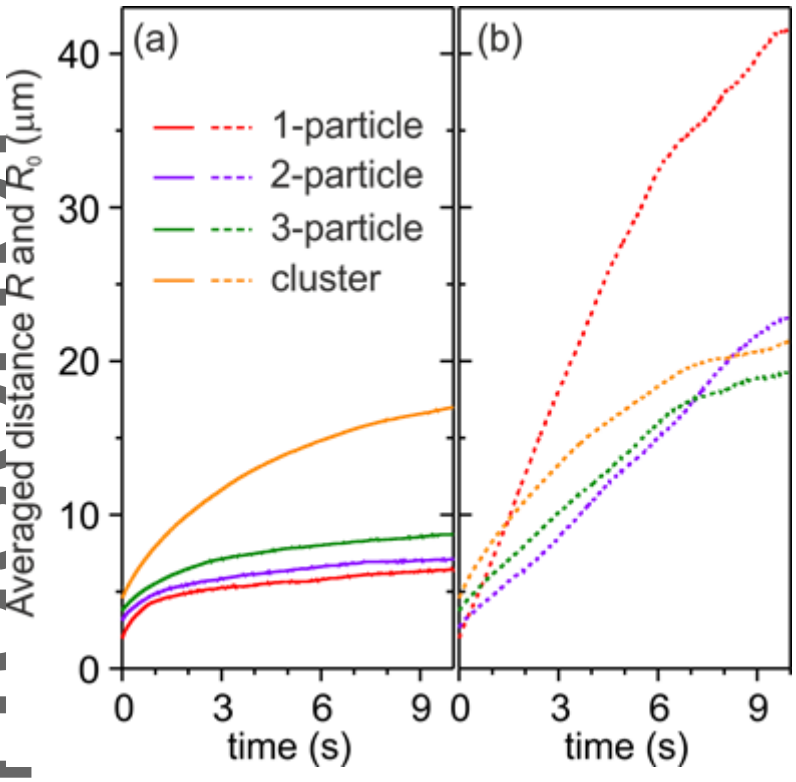

Figure 6. Calculated average distances between PS beads and different Janus particle assemblies (one, two, three particles, and a small cluster). (a) Distance R_0 between a PS bead and the initial position of a Janus object (related to the experimental data shown in Figure 2g, 3g, 4g). (b) Distance R between a PS bead and a Janus object (related to the experimental data shown in Figure 2f, 3f, 4f).

Visible-light-actuated plasmonic Ag/AgCl-based spherical Janus micromotors reveal efficient exclusion effect to surrounding passive beads in pure H_2O. The exclusion efficiency is controlled by the number of single Janus particles composing micromotors. The system-specific interaction parameter between Janus micromotors and passive beads is determined. It assures predictive power for further theoretical analysis of the complex dynamics of these heterogeneous active-passive systems.